applied sciences

MDPI

Communication

Strategic Elements in Holocene Sediments of the Tinto River Estuary (SW Spain)

Verónica Romero [1], Francisco Ruiz [1,*], María Luz González-Regalado [1], Joaquín Rodríguez Vidal [2], Luis Miguel Cáceres [1], Antonio Toscano [1], Paula Gómez [1], Manuel Abad [3], Tatiana Izquierdo [3] and Gabriel Gómez [1]

[1] Departamento de Ciencias de la Tierra, Universidad de Huelva, 21071 Huelva, Spain; vero.ra93@gmail.com (V.R.); montero@dgeo.uhu.es (M.L.G.-R.); mcaceres@dgeo.uhu.es (L.M.C.); antonio.toscano@dgyp.uhu.es (A.T.); paula.gomezgutierrez@hotmail.com (P.G.); ggomezalvarez@yahoo.es (G.G.)
[2] Gibraltar National Museum, Gibraltar GX11 1AA, UK; jrvidal@uhu.es
[3] Departamento de Biología y Geología, Física y Química Inorgánica, Universidad Rey Juan Carlos, 28933 Móstoles, Spain; manuel.abad@urjc.es (M.A.); tatiana.izquierdo@urjc.es (T.I.)
* Correspondence: ruizmu@uhu.es

Abstract: River mouths act as containers for pollution episodes that have occurred in their drainage basins over time. The estuary of the Tinto River is currently one of the most polluted areas in the world, due to past and recent mining and industrial activities. This communication studies the concentrations of seven strategic minerals in a sediment core obtained in the middle estuary of this river. The Holocene geochemical record has allowed us to distinguish four episodes of contamination: an initial one due to acid rock drainage during the MIS-1 transgression and three anthropogenic ones due to the first mining activities, the Roman period, and the industrial mining stages of the 19th and 20th centuries. The concentrations of these strategic minerals increase from the first episode to the fourth. A first evaluation of the concentrations obtained in this core and adjacent pre-Holocene formations reveals that they are too low to consider these sediments ore deposits of the seven elements studied.

Keywords: strategic minerals; pollution; estuary; Holocene; SW Spain

Received: 8 November 2024
Revised: 13 December 2024
Accepted: 26 February 2025
Published: 1 March 2025

Citation: Romero, V.; Ruiz, F.; González-Regalado, M.L.; Rodríguez Vidal, J.; Cáceres, L.M.; Toscano, A.; Gómez, P.; Abad, M.; Izquierdo, T.; Gómez, G. Strategic Elements in Holocene Sediments of the Tinto River Estuary (SW Spain). *Appl. Sci.* **2025**, *15*, 2655. https://doi.org/10.3390/app15052655

1. Introduction

In recent decades, there has been a remarkable socio-economic revolution that has led to a significant increase in the consumption of certain goods, such as computers, mobile phones, cars, televisions, etc. In order to satisfy their demand, a series of chemical elements necessary for their mass production are essential or needed even in small quantities for the specific and vital needs of people and countries. These critical and strategic elements include Al, Be, Li, Mo, Sb, Sc, and Ti, among others [1–3]. Al and Be are critical elements for major world economies, such as the United States, Europe, or Japan [4]. The former has a multitude of applications in daily life (batteries, electrolyzers, data storage and servers, smartphones, tables, laptops, etc.), while the latter has special properties that make it suitable for use in structural aerospace components, jet fighters, or helicopters, and satellites [5]. Li is essential in the production of electric cars, lithium batteries, wind turbines, solar panels, motors, and electrical wiring [6]. Mo and its alloys are of great interest in the aerospace industry and aeronautic fields [7] while some of the main applications of Sb include the manufacture of semiconductors, lead hardeners, diodes, or fire retardants [8].

Sc and Ti are very important in high-tech industries because of their wide application in green, space, and defense technologies [9,10]. Consequently, each country or company must search for these natural elements, and this has led to a substantial increase in the search and extraction of these resources [11,12].

Currently, these strategic elements come from a variety of rocks, sediments, and minerals. Laterite-type bauxites are the most important type of aluminum ore deposits, which are mainly mined in Australia, Guinea, Brazil, Jamaica, and China [13,14]. Beryllium is currently produced from bertrandite (Be_4 Si_2 O_7 $(OH)_2$) and beryl (Be_3 Al_2 Si_6 O_{18}), with the United States as the world's leading producer [15]. The world's largest lithium reserves are concentrated in Chile, Australia, Argentina, and China in both brines and hard rock ores [16], while the latter country is the world's largest producer of molybdenum, obtained mainly from molybdenite (MoO_3) and antimony (54%) [17,18]. Scandium is primarily hosted in magmatic mafic and ultramafic intrusions and its production is still too small (10–15 tons per year) for its growing demand, see review in [19]. Titanium is mainly produced from ilmenite ($FeTiO_3$) and rutile (TiO_2), with world production led by China [20]. China is the largest supplier of these strategic elements to the EU (44%) and, therefore, it is essential to evaluate different rocks and sediments as potential ore deposits in Spain and the rest of the countries that make up the EU to alleviate this significant dependence [21]. As a result, the number of papers and research on this topic has increased significantly in the last decade in Spain, e.g., [22–25].

On the other hand, the concentrations of these elements or their isotopes in surface sediments and Holocene sediment cores extracted from coastal environments (lagoons, estuaries, deltas, shelves) have been used for a set of purposes: (i) the statistical differentiation of depositional (paleo-)environments [26]; (ii) the detection of continental inputs [27]; (iii) the delineation of periods of widespread anoxia in the geologic record [28]; or (iv) identification of past contamination episodes, in conjunction with the concentrations of various metals, such as Cu, Zn, or Pb [29].

This article analyses the content of these seven chemical elements in a sediment core extracted from the middle estuary of the Tinto River (SW Spain). The aim is to make the first evaluation of the use as ores of these strategic elements, as well as to make a comparison between their concentrations in different sedimentary environments deposited during the Neogene and Holocene.

2. Materials and Methods

2.1. Study Area

The Tinto River (101 km length) flows through the southwest of the Iberian Peninsula. It is a typically Mediterranean river, with a variable flow (10- > 100 Hm^3/year) depending on rainfall [30]. This river forms a large mesotidal estuary at its mouth together with the Odiel River into the Atlantic Ocean (Figure 1A,B). This estuary is heavily silted, with wide expanses of marshland, two sandy arrows (Figure 1B: Punta Umbría, Punta Arenillas), and the presence of the island barrier of Saltés that delimits two main outflow channels (Figure 1C: Punta Umbría Channel and Padre Santo Channel). In the middle estuary of this river, several old coves can be distinguished, including the La Fontanilla Cove, located next to the municipality of Palos de la Frontera (Figure 1B,C).

The sedimentary record of this old cove is made up of (i) early Holocene sandy alluvial sediments; (ii) bioclastic sands from marine invasion during the MIS-1 transgression between 6.5 and 5 kyr BP; (iii) clayey silts deposited in tidal channels, lagoons, and marshes; and (iv) a recent sandy filling (Figure 1D) [30].

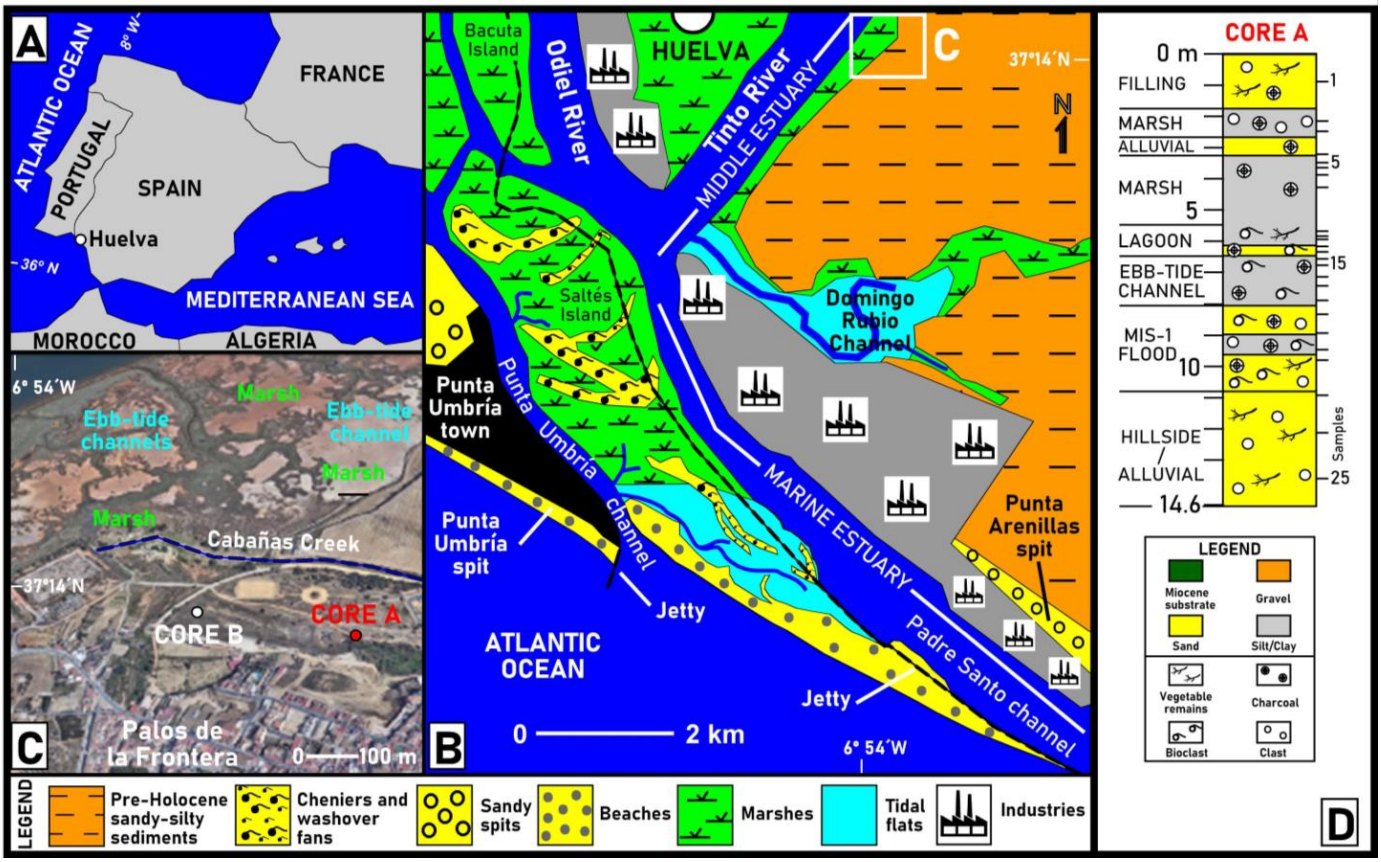

Figure 1. (**A**,**B**) Location and geomorphology of the Tinto–Odiel Estuary, with the situation of La Fontanilla Cove; (**C**) main features of La Fontanilla Cove and location of core A; (**D**) lithostratigraphy, paleoenvironmental reconstruction, sampling, and dating of core A [14].

The Rio Tinto basin includes part of the Iberian Pyrite Belt, one of Europe's major metallogenic provinces, with giant massive sulfide deposits. These sulfide layers have been washed out since the Neogene, causing the first contaminated acid rock drainage event in this estuary during the MIS-1 transgression around 6.5–5 kyr BP. Subsequently, three new peaks of contamination were detected, associated with the first mining works (~5–4.5 kyr BP), the Roman exploitation (~2–1.7 kyr BP), and the intensive exploitation of the 19th and 20th centuries, in conjunction with industrial pollution from two industrial concentrations on the margins of the estuary (Figure 1B; 1960–1990) [31,32]. As a consequence, this river currently shows acid mine drainage phenomena, with a strongly acidic pH [33].

2.2. Sampling and Chemical Analysis

A continuous core (Figure 1D; core A; 14.6 m depth) was obtained in the inner part of La Fontanilla Cove, located in the middle estuary of the Tinto River and in the vicinity of the town of Palos de la Frontera. The location of this core was selected in a relatively protected area to avoid the erosive action of the main channel of the Tinto River during the Holocene as much as possible. A multidisciplinary geological analysis revealed the main sedimentary facies and the paleoenvironmental evolution of this core [31].

Twenty-five samples (2 cm thickness) were extracted from this sedimentary record, ranging from basal alluvial deposits to a recent final anthropogenic fill. These samples were stored in polyethylene bags and kept frozen until chemical analysis. The samples were then ground in an agate mortar for shipping and chemical analysis was carried out using MS Analytical (Langley, BC, Canada). The concentrations of seven strategic elements

(Al, Be, Li, Mo, Sb, Sc, and Ti) were determined by ICP atomic emission spectrometry, with <5% variation between different replicate samples and quality control based on >30 sample references (e.g., OREAS 904). The chemical analysis was performed using the four-acid method (hydrochloric, nitric, perchloric, and hydrofluoric acids) because only the most highly resistant minerals will not be dissolved using this type of digestion. The detection limits were 0.01% for Al and Ti, 0.05 mg kg^{-1} for Be and Mo, 0.2 mg kg^{-1} for Li, 0.5 mg kg^{-1} for Sb, and 0.1 mg kg^{-1} for Sc.

2.3. Dating

Five ^{14}C wood dates were produced at the National Center of Accelerators (CNA, Seville, Spain), with a subsequent calibration using CALIB version 8.2. The final results correspond to calibrated ages using 2σ intervals. These calibrated ages were completed with a comparison between the vertical geochemical variations and the main periods of mining extraction and industrial discharges (see Study Area).

3. Results and Discussion

3.1. Age and Sedimentation Rates

The sedimentary record of core A spans the last 8.4 kyr BP, in agreement with the maximum age of sample A-25, located near its base (Figure 2). The mean sedimentation rate (Figure 2: MSR) was ~2.37 mm yr^{-1} between 8.4 kyr BP and 6.2 kyr BP (sample A-21) and then decreased to 1.05 mm yr^{-1} between 6.2 kyr BP and 4.3 kyr BP (sample A-17). This downward trend became more pronounced between 4.3 kyr BP and 2.2 kyr BP (sample A-13), with an MSR of 0.57 mm yr^{-1}. Finally, it was not possible to calculate this rate in the last 2.2 kyr BP, since the calibration of sample A-8 (-198 ± 98 yr BP) turned out to be subrecent.

During the middle and upper Holocene, these decreasing MSR were measured in other cores from the estuary of the Tinto and Odiel rivers (e.g., Figure 1C: core B), largely due to their progressive siltation and the growth of barrier islands and marshes in their marine sector. About 9 kyr ago, this MSR was ~3 mm yr^{-1} and has decreased to less than 2 mm yr^{-1} in the last 2000 years [34,35].

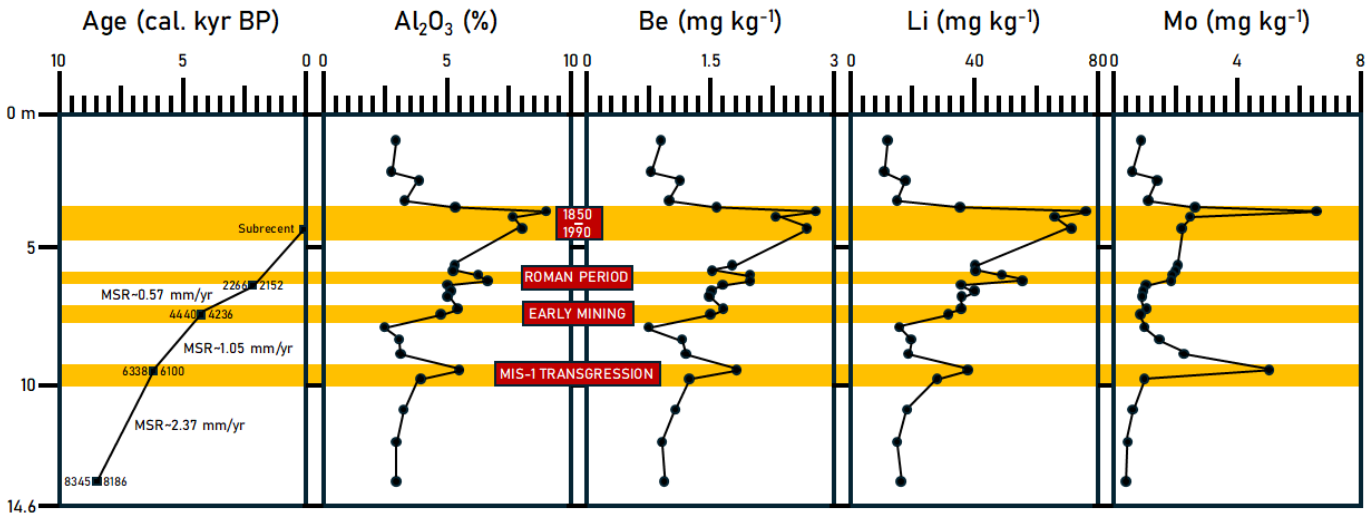

Figure 2. *Cont.*

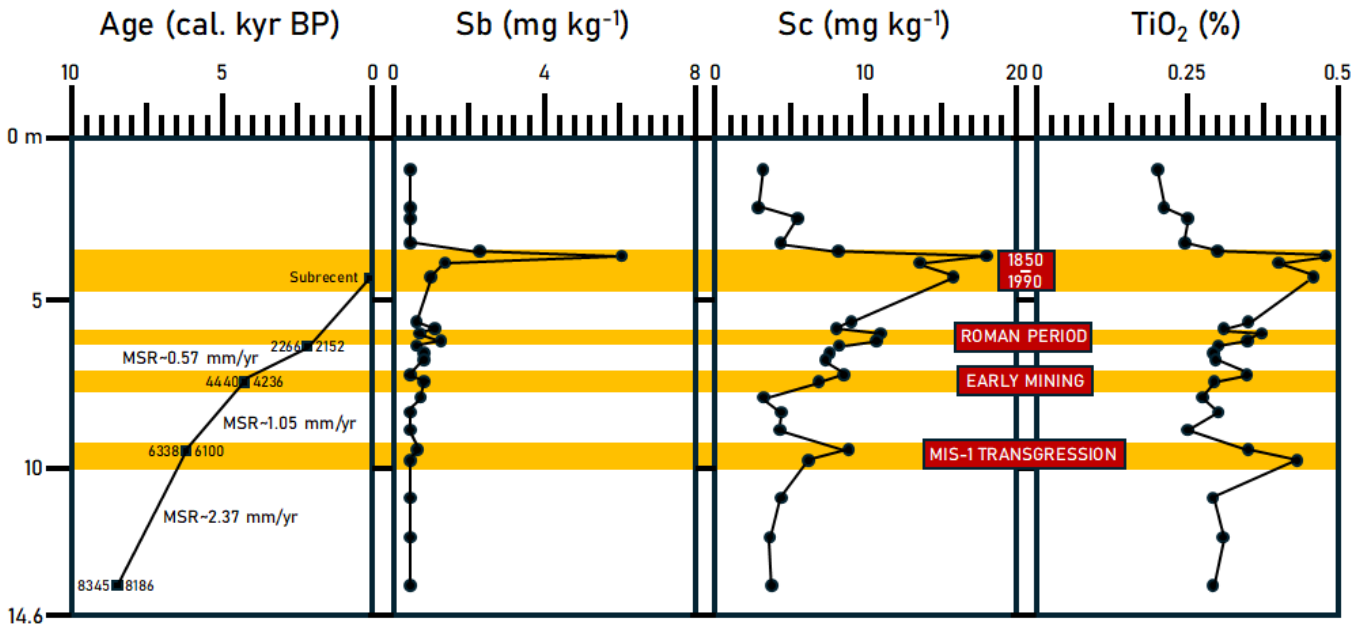

Figure 2. Age model and vertical distribution of strategic elements in core A.

3.2. Strategic Elements and Paleoenvironmental Evolution

The base of core A is composed of sandy alluvial sediments deposited between 8.2 kyr BP and 6.5 kyr BP (Figure 1D: samples A-25 to A-23). They show low-to-very-low average contents of Al (2.93–3.29%; Mean-M-: 3.05%), Be (0.9–1.07 mg kg^{-1}; M: 0.97 mg kg^{-1}), Li (15.2–18.1 mg kg^{-1}; M: 16.3 mg kg^{-1}), Mo (0.38–0.63 mg kg^{-1}; M: 0.48 mg kg^{-1}), Sb (0.5 mg kg^{-1}), Sc (3.6–4.3 mg kg^{-1}; M: 3.9 mg kg^{-1}), and Ti (0.29–0.31%; M: 0.3%) in relation with the rest of the core (Figure 2 and Table 1). These concentrations are similar to those of the upper anthropic filling of core A and other cores obtained in this estuary (Figure 1C), indicating that this filling came from the alluvial materials surrounding La Fontanilla Cove [32].

This cove was flooded during the maximum of the MIS-1 transgression between 6.5 kyr BP and 5.3 kyr BP [36]. In these 1.2 kyr, almost 3 m of bioclastic sands (samples A-22 to A-19) were deposited, with a two-fold increase in the strategic elements around 6.2 kyr BP (Figure 2: sample A-21). This increase came from natural processes such as acid rock drainage, which can be inferred from the chemical concentrations of Pleistocene terraces in the Tinto River [37]. The final phase of this transgression saw a decrease in these concentrations, which reached values similar to those of the underlying alluvial sediments for most of the elements analyzed.

The second peak of strategic elements was marked by the beginning of mining activities in the Iberian Pyritic Belt around 4.4 kyr BP (Figure 2: sample A-17) and by the transition from ebb-tide channels to marshes (Figure 1D). This conjunction led to a remarkable increase in the concentrations of almost all strategic elements (e.g., Al: up to 6.64%; Li: up to 55.2 mg kg^{-1}; Sc: up to 10.9 mg kg^{-1}). This increase coincided with a peak of other elements in the sediment cores of this estuary, such as Cu, Pb, or As [38].

Table 1. Concentrations of strategic elements in core A.

SAMPLE	Al_2O_3 %	Be mg kg^{-1}	Li mg kg^{-1}	Mo mg kg^{-1}	Sb mg kg^{-1}	Sc mg kg^{-1}	TiO_2 %
A-1	2.85	0.91	11.8	0.84	0.5	3.2	0.2
A-2	2.69	0.8	11	0.61	0.5	2.9	0.21
A-3	3.8	1.13	18	1.44	0.5	5.5	0.25
A-4	3.33	1.01	15.2	1.2	0.5	4.3	0.24
A-5	5.35	1.58	35.2	1.12	2.3	8.1	0.3
A-6	8.98	2.78	76	2.65	6.1	17.9	0.48
A-7	7.61	2.3	66	6.57	1.4	13.4	0.4
A-8	7.99	2.67	71.3	2.45	1	15.8	0.46
A-9	5.38	1.73	40.8	2.18	0.6	9	0.35
A-10	5.32	1.54	41.6	2.12	1.1	8.1	0.31
A-11	6.28	1.96	49.2	2.03	0.7	10.9	0.37
A-12	6.64	1.96	55.2	1.86	1.3	10.8	0.35
A-13	4.92	1.66	36.3	1.05	0.6	8.3	0.3
A-14	5.19	1.53	40.5	0.9	0.9	7.6	0.29
A-15	4.96	1.48	36.3	0.83	0.9	7.3	0.29
A-16	5.38	1.66	35.9	1.04	0.5	8.5	0.33
A-17	4.71	1.4	32.1	0.87	0.8	6.8	0.27
A-18	2.5	0.75	16.3	1.02	0.7	3.2	0.25
A-19	3.02	0.98	19.2	1.51	0.5	4.3	0.3
A-20	3.17	1.07	18.6	2.25	0.5	4.2	0.25
A-21	5.51	1.83	38	5.1	0.6	8.8	0.35
A-22	3.95	1.24	27.6	1.06	0.5	6.1	0.43
A-23	3.29	1.07	18.1	0.63	0.5	4.3	0.29
A-24	2.92	0.9	15.2	0.44	0.5	3.6	0.31
A-25	2.93	0.95	15.8	0.38	0.5	3.8	0.29

The peak of the Roman exploitation (2–1.9 kyr BP) led to a further increase in the concentrations of all these elements (Figure 2). This increase was especially significant for Mo (up to 2.03 mg kg^{-1}) and Sb (up to 1.3 mg kg^{-1}), which doubled their concentrations in relation to the underlying sediments. During this period, it is estimated that 25 million tons of pyrite were extracted from the Iberian Pyrite Belt [39].

The last mining activities (1850–1990) and recent industrial wastes (1960–1990) witnessed a fourth peak in strategic elements (samples A-8 to A-6) with the highest concentrations of core A (Figure 2; Al: up to 8.98%; Be: up to 2.78 mg kg^{-1}; Li: up to 76 mg kg^{-1}; Mo: up to 6.57 mg kg^{-1}; Sb: up to 6.1 mg kg^{-1}; Sc: up to 17.9 mg kg^{-1}; Ti: up to 0.48%). Numerous previous studies of sediment cores extracted from the estuary of the Tinto River also show that this pollution episode was the most important in the paleoenvironmental evolution of its basin [40,41].

The progressive siltation of La Fontanilla Cove caused the loss of tidal connection in this inner zone, which explains the low values of strategic minerals in the marshes and alluvial sediments of the upper part of core A (samples A-5 to A-2). Consequently, the distribution of these strategic metals also allows us to detect environmental changes.

3.3. Estuarine Sediments as Ore Deposits?

The background of the seven analyzed elements, obtained from their average concentrations in the Earth's crust (Al: 8.23%; Be: 2.8 mg kg^{-1}; Li: 20 mg kg^{-1}; Mo: 1.2 mg kg^{-1}; Sb: 0.2 mg kg^{-1}; Sc: 22 mg kg^{-1}; Ti: 0.565%), can be used to make a preliminary evaluation of these estuarine sediments as potential ore deposits [42,43]. In an initial review, Al, Be, Sc, and Ti were discarded due to their concentrations being lower than this background in the whole of core A. Lithium concentrations (up to 76 mg kg^{-1}) are clearly lower than those observed in its main deposits located in mines (1–2% Li_2O) or in brines (200–1400 mg kg^{-1}) [44,45], while a similar perspective is obtained when comparing the maximum Mo concentrations (up to 6.57 mg kg^{-1}) with ore deposits from the central United States (0.02–0.36% Mo) [46]. Finally, the Sb concentrations (up to 6.1 mg kg^{-1}) are very low compared to the average percentages of this element in deposits in Russia or China (up to 14%) [47].

3.4. Strategic Elements in Pre-Holocene Sediments from Southwestern Spain: A Preliminary Approach

The abundance of these strategic materials has not been specifically addressed by any study in southwestern Spain, although some papers include some of them in their geochemical data. The last three pollution peaks come from the mining of the Paleozoic polymetallic deposits of the Iberian Pyritic Belt, exploited in several dozen mines. The geochemical analysis of some of these deposits and residual soils includes some of the elements studied in this paper, such as Al (up to 0.01–16.1%), Be (up to 8.9 mg kg^{-1}), Li (3.3–400 mg kg^{-1}), Mo (up to 26,700 mg kg^{-1}), Sc (0.5–53,5 mg kg^{-1}), or Ti (up to 1.19%) [48,49]. However, this millenary mining has focused on polymetallic sulfides or precious metals and not specifically on these elements [50].

The Gibraleón Clay Formation [51] is the most widespread Neogene geological unit in the vicinity of the estuary of the Tinto and Odiel rivers. These upper Miocene silty-clay materials show Al values between 4% and 5% in some cores obtained in the Tinto River [35] and do not reach 3 ppm of Be in the sandiest levels of this formation [52]. The Pliocene glauconitic levels of the overlying Huelva Sand Formation [51] have Al contents between 5% and 6% [53], while the Pleistocene terraces of the Tinto River show values lower than 9% in Al and 0.5% in Ti [37]. This first approximation would indicate that all these materials are not suitable for the economic extraction of these strategic minerals.

4. Conclusions

1. The geochemical analysis of a sediment core extracted from the middle estuary of the Tinto River (SW Spain) revealed that the strategic elements studied (Al, Be, Li, Mo, Sb, Sc, and Ti) can be considered markers of the pollution episodes (one natural and three anthropogenic) that have occurred in this area during the Holocene.
2. A natural acid rock drainage occurred during the MIS-1 transgression (6.2 kyr BP), followed by two episodes of mining-related contamination around 4.4 kyr BP and 2–1.9 kyr BP.
3. The main pollution episode is associated with mining activities (1850–1990) and industrial discharges (1960–1990) in recent years.
4. These estuarine sediments and other pre-Holocene formations and terraces do not serve as ores of these elements due to their very low concentrations in relation to those obtained in current mines in various parts of the world.

Author Contributions: All authors have participated in all stages of the paper. All authors have read and agreed to the published version of the manuscript.

Funding: This study was mainly financed by the Palos de la Frontera Council. It was also carried out through the following projects: (a) DGYCIT project CTM2006-06722/MAR; (b) DGYCIT project CGL2006-01412; (c) Roman cities of the Baetica, CORPVS VRBIVM BAETICARVM (I) (CUB) (Andalusian Government); (d) From the Atlantic to the Tyrrhenian, the Hispanic ports and their commercial relations with Ostia Antica, DEATLANTIR II—HAR2017-89154-P (Plan Nacional de I + D + i); and (e) FEDER 2014–2020 project UHU-1260298. Other funds were provided by the Andalusian Government (groups HUM-132, RNM-238, and RNM-293). This work is a contribution to the Research Center in Historical, Cultural and Natural Heritage (CIPHCN) of the University of Huelva.

Institutional Review Board Statement: Not applicable.

Informed Consent Statement: Not applicable.

Data Availability Statement: Data are available upon request to the corresponding author.

Conflicts of Interest: The authors declare no conflicts of interest.

References

1. Hayes, S.M.; McCullough, E.A. Critical minerals: A review of element trends in comprehensive critical studies. *Resour. Policy* **2018**, *59*, 192–199. [CrossRef]
2. Kamran, M.; Raugei, M.; Hutchinson, A. Critical elements for a successful energy transition: A systematic review. *Renew. Sustain. Energy Transit.* **2023**, *4*, 100068. [CrossRef]
3. Silva, G.F.; Silva, A.D.R.; Souza Gaia, S.M. *An Overview of Critical and Strategic Minerals of Brazil*; Serviço Geológico do Brasil: Brasília, Brazil, 2024; 35p.
4. Su, Y.; Hu, D. Global Dynamics and Reflections on Critical Minerals. *E3S Web Conf.* **2022**, *352*, 03045. [CrossRef]
5. Carrara, S.; Bobba, S.; Blagoeva, D.; Alves Dias, P.; Cavalli, A.; Georgitzikis, K.; Grohol, M.; Itul, A.; Kuzov, T.; Latunussa, C.; et al. *Supply Chain Analysis and Material Demand Forecast in Strategic Technologies and Sectors in the EU—A Foresight Study*; Publications Office of the European Union: Luxembourg, 2023. [CrossRef]
6. Bedoya Londoño, J.A.; Franco Sepúlveda, G.; De la Barra Olivares, E. Strategic Minerals for Climate Change and the Energy Transition: The Mining Contribution of Colombia. *Sustainability* **2024**, *16*, 83. [CrossRef]
7. Kuang, Z. Molybdenum and its alloys in advanced engine applications: From material selection to surface optimization. *E3S Web Conf.* **2024**, *560*, 02016. [CrossRef]
8. Bagherifam, S.; Brown, T.C.; Wijayawardena, A.; Naid, R. The influence of different antinomy (SB) compounds and ageing on bioavailability and fractionation of antimony in two dissimilar soils. *Environ. Pollut.* **2021**, *270*, 116270. [CrossRef]
9. Schulz, K.J.; DeYoung, J.H., Jr.; Bradley, D.C.; Seal, R.R. Critical mineral resources of the United States—An introduction. In *Critical Mineral Resources of the United States—Economic and Environmental Geology and Prospects for Future Supply*; Schulz, K.J., DeYoung, J.H., Jr., Seal, R.R., II, Bradley, D.C., Eds.; U.S. Geological Survey Professional Paper 1802; U.S. Geological Survey: Reston, VA, USA, 2017; pp. A1–A14. [CrossRef]
10. Kumar, S.; Haque, N.; Bhuiyan, M.; Bruckard, W.; Pramanik, B.K. Recovery of strategically important critical minerals from mine tailings. *J. Environ. Chem. Eng.* **2022**, *10*, 107622. [CrossRef]
11. Sryrvatka, V.; Rabets, A.; Gromyko, O.; Luzhetskyy, A.; Fedorenko, V. Scandium-microorganism interactions in new biotechnologies. *Trends Bibtechnol.* **2022**, *40*, 1088–1101. [CrossRef]
12. Najafizadeh, M.; Yazdi, S.; Bozorg, M.; Ghasempour-Mouziraji, M.; Hosseinzadeh, M.; Zarrabian, M.; Cavaliere, P. Classification and applications of titanium and its alloys: A review. *J. Alloys Compd. Commun.* **2024**, *3*, 100019. [CrossRef]
13. Chen, J.; Peng, D. Management and disposal of alumina production wastes. In *Managing Mining and Minerals Processing Wastes. Concepts, Design and Applications*; Qi, C., Benson, C.H., Eds.; Elsevier: Amsterdam, The Netherlands, 2023; pp. 133–163. [CrossRef]
14. Meyer, F.M. Availability of bauxite reserves. *Nat. Resour. Res.* **2004**, *13*, 161–172. [CrossRef]
15. Lederer, G.W.; Foley, N.K.; Jaskula, B.W.; Ayuso, R.A. *Beryllium—A Critical Mineral Commodity—Resources, Production, and Supply Chain*; Fact Sheet 2016–3081; U.S. Geological Survey: Reston, VA, USA, 2016. Available online: https://pubs.usgs.gov/fs/2016/3081/fs20163081.pdf (accessed on 30 September 2024).
16. Gil-Alana, L.-A.; Monge, M. Lithium: Production and estimated consumption. Evidence of persistence. *Resour. Policy* **2019**, *60*, 198–202. [CrossRef]
17. Liu, B.; Zhang, B.; Han, G.; Wang, M.; Huang, Y.; Su, S.; Xue, Y.; Wang, Y. Clean separation and purification for strategic metals of molybdenum and rhenium from minerals and waste allí scraps—A review. *Resour. Conserv. Recycl.* **2022**, *181*, 106232. [CrossRef]

18. Kanellopoulos, C.; Sboras, S.; Voudouris, P.; Soukis, K.; Moritz, R. Antimony's significance as a critical metal: The global perspective and the Greek deposits. *Minerals* **2024**, *14*, 121. [CrossRef]
19. Wang, Z.; Li, M.Y.H.; Liu, Z.R.; Zhou, M. Scandium: Ore deposits, the pivotal role of magmatic enrichment and future exploration. *Ore Geol. Rev.* **2021**, *128*, 103906. [CrossRef]
20. El Khalloufi, M.; Drevelle, O.; Soucy, G. Titanium: An Overview of Resources and Production Methods. *Minerals* **2021**, *11*, 1425. [CrossRef]
21. European Commission: Directorate-General for Internal Market, Industry, Entrepreneurship and SMEs; Blengini, G.; El Latunussa, C.; Eynard, U.; Torres De Matos, C.; Wittmer, D.; Georgitzikis, K.; Pavel, C.; Carrara, S.; Mancini, L.; et al. *Study on the EU's List of Critical Raw Materials (2020)—Final Report*; Publications Office of the European Union: Luxembourg, 2020. Available online: https://data.europa.eu/doi/10.2873/11619 (accessed on 30 September 2024).
22. Ministry for the Ecological Transition and the Demographic Challenge. *Road Map for the Sustainable Managements of Mineral Raw Materials*; Ministry for the Ecological Transition and the Demographic Challenge: Madrid, Spain, 2022. Available online: https://www.miteco.gob.es/content/dam/miteco/es/ministerio/planes-estrategias/materias-primas-minerales/roadmapforthesustainablemanagementofmineralrawmaterials_tcm30-561498.pdf (accessed on 30 September 2024).
23. Rosario-Beltré, A.J.; Sánchez-España, J.; Rodríguez-Gómez, V.; Fernández-Naranjo, F.J.; Bellido-Martín, E.; Adánez-Sanjuán, P.; Arranz-González, J.C. Critical Raw Materials recovery potential from Spanish mine wastes: A national-scale preliminary assessment. *J. Clean. Prod.* **2023**, *407*, 137163. [CrossRef]
24. Urdangaray, A.; García, E.; Pous, J.; Ortega, M.F.; Mora, P. A stydy on potential lithium extraction in Spain. *Dyna* **2023**, *98*, 215–217. [CrossRef]
25. Sánchez-García, T. *Aluminum in Spain: Mineral Deposits and Mining Production*; Instituto Geológico y Minero de España: Madrid, Spain, 2021. Available online: https://asgmi.org/wp-content/uploads/2021/08/ASGMI_Aluminum-in-SPAIN.pdf (accessed on 30 September 2024).
26. Muhammed, D.D.; Simon, N.; Utley, J.E.P.; Verhagen, I.T.E.; Duller, R.A.; Griffiths, J.; Wooldridge, L.J.; Worden, R.H. Geochemistry of Sub-Depositional Environments in Estuarine Sediments: Development of an Approach to Predict Palaeo-Environments from Holocene Cores. *Geosciences* **2022**, *12*, 23. [CrossRef]
27. Marco-Barba, J.; Burjachs, F.; Reed, J.M.; Santisteban, C.; Usera, J.M.; Alberola, C.; Expósito, I.; Guillem, J.; Patchett, F.; Vicente, E.; et al. Mid-Holocene and historical palaeoecology of the Albufera de València coastal lagoon. *Limnetica* **2019**, *38*, 353–389. [CrossRef]
28. Scholz, F.; Siebert, C.; Dale, A.W.; Frank, M. Intense molybdenum accumulation in sediments underneath a nitrogenous water column and implications for the reconstruction of paleo-redox conditions based on molybdenum isotopes. *Geochim. Cosmochim. Acta* **2017**, *213*, 400–417. [CrossRef]
29. Ruiz, F.; Borrego, J.; López-González, M.; Abad, M.; González-Regalado, M.L.; Carro, B.; Pendón, J.G.; Rodríguez Vidal, J.; Cáceres, L.M.; Prudencio, M.I.; et al. The geological record of a mid-Holocene marine storm. *Geobios* **2007**, *40*, 689–699. [CrossRef]
30. Olías, M.; Nieto, J.M.; Miguel, A.; Ruiz, C. *La Contaminación Minera de los Ríos Tinto y Odiel*; Universidad de Huelva: Huelva, Spain, 2010; 166p.
31. Arroyo, M.; Ruiz, F.; González-Regalado, M.L.; Rodríguez Vidal, J.; Cáceres, L.M.; Olías, M.; Campos, J.M.; Fernández, L.; Abad, M.; Izquierdo, T.; et al. Natural and anthropic pollution episodes during the Late Holocene evolution of the Tinto River estuary (SW Spain). *Sci. Mar.* **2021**, *85*, 113–123. [CrossRef]
32. Arroyo, M.; Ruiz, F.; Campos, J.M.; Bermejo, J.; González-Regalado, M.L.; Rodríguez Vidal, J.; Cáceres, L.M.; Olías, M.; Abad, M.; Izquierdo, T.; et al. Where did Christopher Columbus start?: The estuarine scenario of a historical date. *Estuar. Coast. Shelf Sci.* **2021**, *250*, 107162. [CrossRef]
33. Carro, B.; Borrego, J.; López-González, N.; Grande, J.A.; Gómez, T.; De la Torre, M.; Valente, T. Impact of Acid Mine Drainage on the hydrogeochemical characteristics of the Tinto-Odiel Estuary (SW Spain). *J. Iber. Geol.* **2011**, *37*, 87–96. [CrossRef]
34. Lario, J.; Zazo, C.; Goy, J.L.; Dabrio, C.J.; Borja, F.; Silva, P.G.; Sierro, F.J.; González, A.; Soler, V.; Yll, E. Changes in sedimentation trends in SW Iberia Holocene estuaries (Spain). *Quat. Int.* **2002**, *93–94*, 171–176. [CrossRef]
35. Abad, M.; Arroyo, M.; Ruiz, F.; González-Regalado, M.L.; Rodríguez Vidal, J.; Cáceres, L.M.; Izquierdo, T.; Toscano, A.; Gómez, P.; Gómez, G.; et al. Miocene-Holocene paleoenvironmental changes in the Tinto River estuary (SW Spain) evidenced by sedimentology, geochemistry and fauna. *Carnets Geol.* **2022**, *22*, 825–845. [CrossRef]
36. Dabrio, C.J.; Zazo, C.; Sierro, F.J.; Borja, F.; Lario, J.; González, J.A.; Flores, J.A. Depositional history of estuarine infill during the last postglacial transgression (Gulf of Cadiz, Southern Spain). *Mar. Geol.* **2000**, *162*, 381–404. [CrossRef]
37. Cáceres, L.M.; Olías, M.; de Andrés, J.R.; Rodríguez-Vidal, J.; Clemente, L.; Galván, L.; Medina, B. Geochemistry of Quaternary sediments in terraces of the Tinto River (SW Spain): Paleoenvironmental implications. *Catena* **2013**, *101*, 1–10. [CrossRef]
38. Leblanc, M.; Morales, J.A.; Borrego, J.; Elbaz-Poulichet, F. 4500-year-old mining pollution in southwestern Spain: Long-term implications for modern mining pollution. *Econ. Geol.* **2000**, *95*, 655–662. [CrossRef]

39. Olías, M.; Nieto, J.M. El impacto de la minería en los ríos Tinto y Odiel a lo largo de la historia. *Rev. Soc. Geológica España* **2012**, *25*, 177–192.
40. Davis, R.A.; Welty, A.T.; Borrego, J.; Morales, J.A.; Pendón, J.G.; Ryan, J.G. Río Tinto estuary (Spain): 5000 years of pollution. *Environ. Geol.* **2000**, *39*, 1107–1116. [CrossRef]
41. Olías, M.; Nieto, J.M. Background conditions and mining pollution throughout history in the río Tinto (SW Spain). *Environments* **2015**, *2*, 295–316. [CrossRef]
42. Greenwood, N.N.; Earnshaw, A. *Chemistry of the Elements*; Butterworth-Heinemann: Oxford, UK, 1997.
43. Lide, D.R. *CRC Handbook of Chemistry and Physics*; Taylor & Francis Group: Boca Raton, FI, USA, 2008.
44. Gruber, P.W.; Medina, P.A.; Keoleian, G.A.; Kesler, S.E.; Everson, M.P.; Wallington, T.J. Global Lithium Availability. *J. Ind. Ecol.* **2011**, *15*, 760–775. [CrossRef]
45. Warren, I. Techno-Economic Analysis of Lithium Extraction from Geothermal Brines. Golden, CO: National Renewable Energy Laboratory. NREL/TP-5700-79178, 2021. Available online: https://www.nrel.gov/docs/fy21osti/799178.pdf (accessed on 30 September 2024).
46. Worthington, J. *Porphyry and Other Molybdenum Deposits of Idaho and Montana*; Idaho Geological Survey: Boise, Idaho, 2007; Technical Report 07-3.
47. Schulz, K.J.; De Young, J.H.; Seal, R.R.; Bradley, D. *Critical Mineral Resources of the United States—Economic and Environmental Geology and Prospects for Future Supply*; Professional Paper 1802–C; U.S. Department of the Interior, U.S. Geological Survey: Reston, VA, USA, 2017. [CrossRef]
48. Martín, T.; Martín, S.; Gómez-Ortiz, D.; De Ignacio, C.; Lillo, J. A Geochemical and Geophysical Characterization of Sulfide Mine Ponds at the Iberian Pyrite Belt (Spain). *Water Air Soil Pollut.* **2011**, *217*, 387–405. [CrossRef]
49. Martín-Mendez, I.; llamas, J.; Bel-lan, A.; Locutura, J. Geochemical distribution in residual soils of Iberian Pyrite Belt (Spain). *J. Iber. Geol.* **2023**, *49*, 97–114. [CrossRef]
50. Tornos, F. La Geología y Metalogenia de la Faja Pirítica Ibérica. *Macla* **2008**, *10*, 13–23.
51. Civis, J.; Sierro, F.J.; González Delgado, J.A.; Aores, J.A.; Andrés, l.; de Porta, J.; Valle, M.E. El Neógeno marino de la provincial de Huelva: Antecedentes y definición de las unidades litoestratigráficas. In *Paleontología del Neógeno de Huelva (W. Cuenca del Guadalquivir)*; Universidad de Salamanca: Salamanca, Spain, 1987; pp. 9–21. Available online: https://gredos.usal.es/bitstream/handle/10366/127804/DGL_UnidadesLitoestratigraficas.pdf?sequence=1&isAllowed=y (accessed on 30 September 2024).
52. Romero, V.; Toscano, A.; Ruiz, F.; González-Regalado, M.L.; Abad, M.; Izquierdo, T.; Rodríguez Vidal, J.; Cáceres, L.M.; Marques, R.; Prudencio, M.I.; et al. Análisis geológico multidisciplinar de la Unidad Arenas de Trigueros (Formación Arcillas de Gibraleón, S.O. de España). *Estud. Geológicos* **2023**, *79*, e154. [CrossRef]
53. Galán, E.; González, I.; Mayoral, E.; Vázquez, M.A. Caracterización y origen de la facies glauconítica de la cuenca del Guadalquivir. *Estud. Geológicos* **1989**, *45*, 169–175. [CrossRef]